

ment was to search for nitrogen in the atmosphere of Mars. This first analysis shows no evidence of nitrogen emissions in the ultraviolet spectrum of the upper atmosphere. The following emissions were searched for and found missing: second-positive and Lyman-Birge-Hopfield bands of molecular nitrogen, first-negative bands of ionized molecular nitrogen, gamma bands of nitric oxide, and 1200- and 1493-Å lines of atomic nitrogen. The final analysis of these data will allow

an upper limit to be placed on the amount of nitrogen in the upper atmosphere of Mars.

Repetitive spectra were taken as the Mariner spectrometer crossed the limb of Mars. These data, which contain information about the scale height of individual spectral emissions will be used to construct a model of the Mars upper atmosphere. This first report is simply a record of our identifications in the ultraviolet spectrum of the upper atmosphere. The instrument also ob-

tained spectra of the bright and dark parts of the disc, the terminator, and the atomic hydrogen corona.

C. A. BARTH

*Department of Astro-Geophysics and Laboratory for Atmospheric and Space Physics, University of Colorado, Boulder 80302*

W. G. FASTIE

*Department of Physics, Johns Hopkins University, Baltimore, Maryland 21218*

C. W. HORD, J. B. PEARCE

K. K. KELLY, A. I. STEWART  
G. E. THOMAS, G. P. ANDERSON  
*Department of Astro-Geophysics and Laboratory for Atmospheric and Space Physics, University of Colorado*

O. F. RAPER

*Space Sciences Division, Jet Propulsion Laboratory, Pasadena, California 91103*

#### References and Notes

1. C. A. Barth, *Appl. Optics* **8**, 1295 (1969).
2. —, in *The Middle Ultraviolet—Its Science and Technology*, A. E. S. Green, Ed. (Wiley, New York, 1966); W. G. Fastie, H. M. Crosswhite, D. F. Heath, *J. Geophys. Res.* **69**, 4129 (1964); C. A. Barth, *ibid.*, p. 3301; C. A. Barth and J. B. Pearce, *Space Res.* **6**, 381 (1966); unpublished results from a rocket flight, 13 June 1969.
3. The success of this experiment, which has been under preparation for 9 years, is the result of the efforts of a large number of people at NASA headquarters, the Jet Propulsion Laboratory, the University of Colorado, Johns Hopkins University, and elsewhere in the scientific community. The large scientific return from the Mariner 1969 mission is due to the technical and managerial skills of H. M. Schurmeier and the Mariner project staff at JPL and NASA headquarters. Supported by NASA under JPL contract 951790 and NASA grant NGL 06-003-052.

15 August 1969

#### Jadeite: Shock-Induced Formation from Oligoclase, Ries Crater, Germany

*Abstract. Jadeite (high-pressure sodium aluminum pyroxene) has been identified in a shock-phase assemblage of oligoclase. The shock assemblage consists of minute particles with high refractive indices that contain at least two phases: one (identified by x-ray) is a jadeite that is nearly pure  $\text{NaAlSi}_2\text{O}_6$ ; the other has the chemical composition of oligoclase minus jadeite and appears to be largely amorphous.*

Jadeite has been identified as the major crystalline constituent of a shock-phase assemblage formed by the breakdown of sodic feldspar. Because plagioclase is the most widespread of the common rock-forming minerals, shock

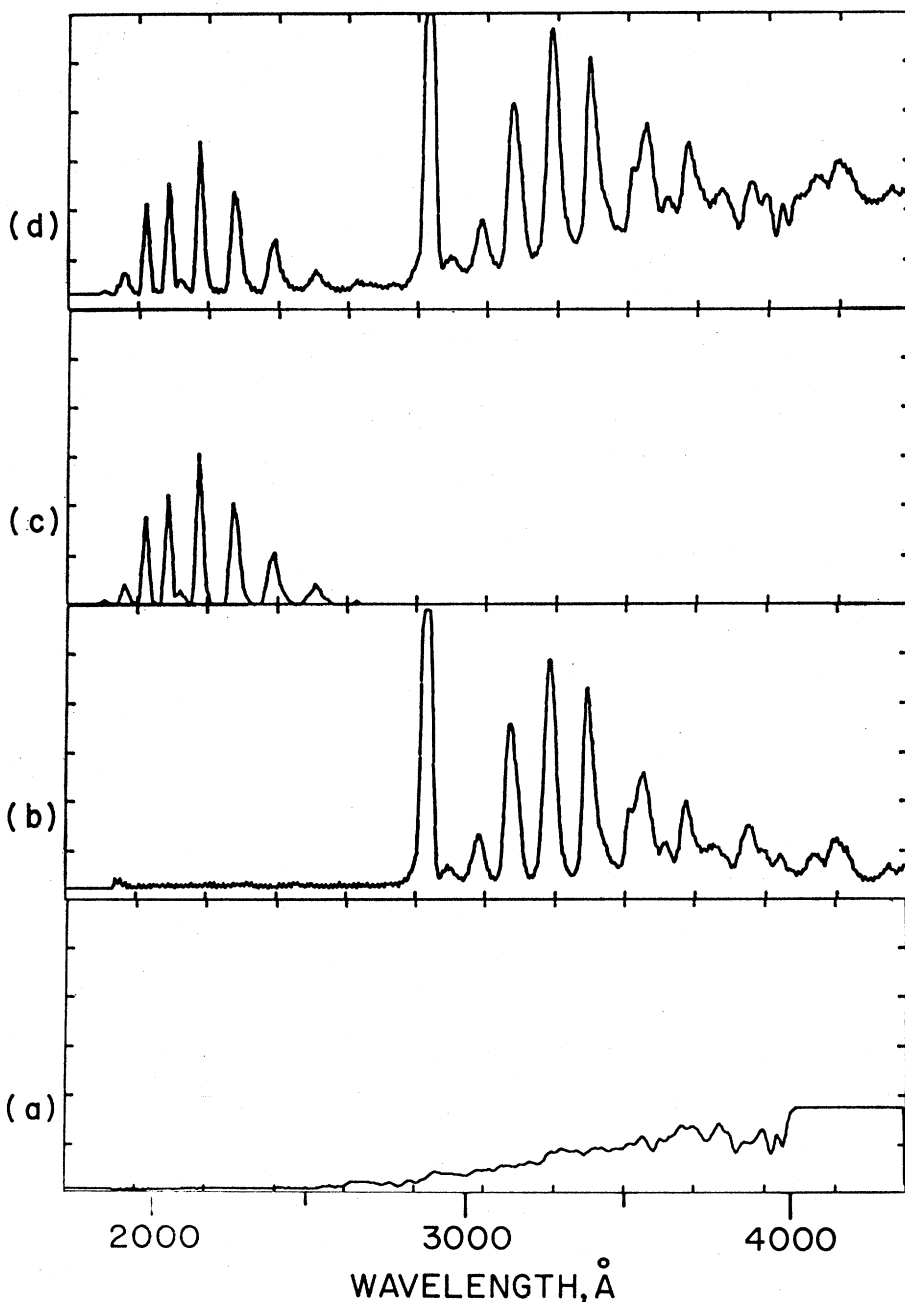


Fig. 2. Synthesis of comparison spectrum. (a) Off-axis light component from Mars disc. (b) Carbon dioxide spectrum from laboratory electron impact experiment. (c) Carbon monoxide spectrum from theoretical calculation of fluorescence scattering. (d) Composite spectrum synthesized by adding a, b, and c.

conversion of this mineral to jadeite is relevant to studies of lunar rock samples as well as to studies of rocks from terrestrial impact or explosion structures.

The phase assemblage containing jadeite forms small particles in maskelynite [thetomorphic plagioclase glass (1)] in several specimens of impact-metamorphosed amphibolite from the Ries Crater, Germany (2). The shock effects in most of these specimens are similar: tectosilicates have been converted to amorphous and high-pressure crystalline phases, mafic minerals retain their original crystal structures, and rock texture is strikingly preserved. Quartz is converted to thetomorphic

silica glass containing minor amounts of coesite. Plagioclase is converted to thetomorphic glass that contains jadeite-bearing particles, spherules and patches of montmorillonite, spherules of secondary calcite, and abundant arcuate fractures.

In the amphibolite sample selected for study, maskelynite grains have refractive indices ranging from 1.5009 to 1.5123 ( $\pm 0.0002$ ); electron microprobe analysis indicates that the glass is of oligoclase composition (72 mole percent albite, 22 mole percent anorthite, and 6 mole percent orthoclase), and is homogeneous to within  $\pm 1$  percent anorthite. The jadeite-bearing particles embedded in the maskelynite are

1 to 5  $\mu\text{m}$  in diameter, have a relatively high refractive index of  $1.585 \pm 0.015$  (3), and tend to be distributed in irregular stringers (Fig. 1). In some grains the stringers are regular and apparently parallel to crystal planes of the original feldspar.

With the petrographic microscope the jadeite-bearing particles can be barely resolved into two or more components; an electron microscope was used to investigate the fine structure within the particles. Grains of maskelynite containing particles with high refractive indices were mounted in epoxy, and their surfaces were ground and polished. The polished surfaces were etched for 3 seconds in vapor from 48 percent HF. Thick negative replicas of polyvinyl alcohol were made from the surfaces of selected grains; these were preshadowed with platinum and carbon and were given a thin coat of evaporated carbon. The polyvinyl alcohol replicas were then dissolved in water, and the remaining positive platinum-shadowed carbon replicas were examined with an electron microscope. The electron micrographs of the particles (Fig. 2) show at least two phases, one resistant to HF and one or more etched by HF. The etched areas form stringers of minute subparticles within the resistant phase; these subparticles average about 0.1  $\mu\text{m}$  in diameter and make up roughly half the volume of the particles (estimated by point count from several micrographs). Comparison of observations made with the petrographic and electron microscopes shows that the phase resistant to HF is of higher refractive index and reflectivity than the etched phase.

Several single grains of maskelynite containing an abundance of particles with high refractive indices were each mounted on glass fibers with silicone grease, and Debye-Scherrer powder patterns were taken in cameras of 57.3- and 114.6-mm diameters with  $\text{CuK}\alpha$  radiation on a microfocuss x-ray generator. The grains yield weak powder patterns of jadeite— $\text{NaAlSi}_2\text{O}_6$ , a high-pressure sodium aluminum pyroxene (4). In the best pattern obtained from a single grain (Table 1), 22 jadeite lines can be distinguished (the only lines on the pattern not attributable to jadeite are the strong line of calcite and two weak streaky lines with  $d$ -spacings of 2.71 and 2.34  $\text{\AA}$ ). On all the powder patterns the jadeite lines are sharp and continuous, thus indicating a grain size of about 0.1 to 1

Table 1. The  $d$ -spacings of Ries, synthetic, and Burma jadeites. The listing of  $d$ -spacings for jadeite in untreated maskelynite is the complete pattern. The listing for acid-treated jadeite consists only of lines not interfered with by lines of platinum and fluosilicates introduced in acid treatment; the listing for synthetic jadeite consists of the lines equivalent to those measured in the acid-treated Ries sample. The listing of  $d$ -spacings for Burma jadeite, determined by film measurements (6), is given for comparison. Table 2 presents cell parameters calculated from starred reflections (Table 1).

$hkl$ †	Ries							
	Untreated maskelynite‡		Concentrate treated with HF and HCl‡		Synthetic‡§		Burma	
	$d$ (Å)	$I$	$d$ (Å)	$I$	$d$ (Å)	$I$	$d$ (Å)	$I$
110							*6.19	40
111	4.32	25						
020							*4.29	80
021	3.24	18					*3.25	50
220	3.10	18					*3.11	50
221	2.93	100	*2.92	100	*2.92	100	*2.92	100
311, 310	2.84	50	2.83	50	2.83	71	2.82	100
002, 131	2.49	50	2.49	50	2.49	50	2.50	80
221	2.42	35	*2.42	35	*2.42	35	*2.42	80
400							2.24	60
222, 312 }	2.21	13					2.19	60
112	2.16	25	*2.16	35	*2.16	25		
331, 330	2.07	18	2.068	25	2.069	25	2.069	70
421			*2.047	6	*2.048	4		
041	1.97	9					*1.971	60
241	1.88	6					*1.892	30
510, 132	1.76	9	1.763	9	1.760	9	1.761	50
150	1.69	6					*1.687	50
313	1.65	9	*1.651	13	*1.653	4	*1.656	20
042							*1.623	20
223	1.61	13	*1.610	9	*1.611	9	*1.613	20
441							*1.577	60
531	1.57	13	*1.573	13	*1.572	13		
440			*1.554	6	*1.551	6	*1.553	50
600, 602							1.508	30
423							*1.484	30
133	1.48	13	*1.478	13	*1.479	13		
260, 531, 152	1.37	6	1.363	9	1.361	9		
314			*1.284	6	*1.283	3		
262, 062	1.24	9	1.242	9	1.240	6		
352	1.20	6	*1.201	6	*1.199	4		

† Generated by computer for each mineral with the cell parameters calculated from the measured  $2\theta$  or  $d$  values. ‡ Patterns of Ries and synthetic jadeites taken with film, in a camera with a diameter of 114.6 mm, with  $\text{CuK}\alpha$  radiation ( $\lambda = 1.5418 \text{ \AA}$ ) and a Ni filter. Lower limit of  $2\theta$  measurable: about  $7^\circ$ , or 12.6  $\text{\AA}$ . § Synthesized at 37.5 kb and 1350°C by P. M. Bell.

$\mu\text{m}$ . In addition, most patterns show spotty and streaky lines produced by calcite, montmorillonite, and unidentified alteration products (5).

A sample (about 15 mg) of maskelynite was treated with concentrated HCl and dilute HF to concentrate the jadeite. The sample was warmed in concentrated HCl in a platinum crucible for 5 minutes to dissolve secondary calcite and was then treated with a mixture of equal parts of 4.8 percent HF and concentrated HCl for 1 hour. After the residue had been washed in warm water, dried, and transferred with silicone grease to the end of a glass fiber, a powder pattern was taken. In Table 1 the  $d$ -spacings of jadeite lines of the pattern are compared with those of synthetic jadeite and jadeite from Burma (6); cell parameters calculated from the  $d$ -spacings (7) are compared with corresponding values for synthetic jadeite and jadeite from Burma in Table 2. The  $d$ -spacings and unit cell do not differ from those of the other jadeites (within the margin of error of the measurements).

The x-ray data indicate that jadeite is the only crystalline phase present in large amounts within the particles with high refractive index. Since the jadeite is concentrated by treatment with HF, this mineral is clearly the phase resistant to HF observed with the electron microscope (Fig. 2). The nature of the material etched by HF is not as easily determined. X-ray studies have revealed no crystalline phases in

Table 2. Cell parameters of Ries (concentrate treated with HF and HCl), synthetic, and Burma jadeites calculated from the starred reflections (Table 1). Estimated accuracy is  $\pm 0.015 \text{ \AA}$ .

Jadeite	$a$ ( $\text{\AA}$ )	$b$ ( $\text{\AA}$ )	$c$ ( $\text{\AA}$ )	$\beta$
Ries	9.44	8.58	5.23	107°32'
Synthetic	9.44	8.56	5.23	107°43'
Burma	9.43	8.58	5.23	107°31'

this material, and shock-produced minerals may be present only in quantities or grain sizes below the detection limits of the techniques employed. Estimates of mean refractive indices of several shock assemblages which might have formed from the oligoclase do, however, set limits on the amount of very fine-grained crystalline products which can be present. If it is assumed that the jadeite is pure  $\text{NaAlSi}_3\text{O}_6$  and that the etched material consists of small ordered domains of quartz, anorthite, and orthoclase, the mean refractive index of the assemblage (8) should be 1.610. This value is much above the observed value of 1.585. If, instead, the etched material consists of a mixture of finely crystalline feldspars and "normal" silica glass, the mean refractive index (8) should be 1.589. On the other hand, if it is assumed that the jadeite is not pure and contains  $\text{CaAl}_2\text{SiO}_6$  in solid solution in the same ratio of Na to Ca as in the original oligoclase, and that the etched material is fine-grained quartz, albite, anorthite, and orthoclase, the mean refractive index (8)

should be 1.605. If, instead, the etched material is a mixture of finely crystalline feldspars and "normal" silica glass, the mean refractive index (8) should be 1.583. Substitution of shock-produced silica glass for "normal" silica glass in these assemblages would increase the predicted indices, as the amorphous glass generally has higher values of density and refractive index than those of "normal" glass (9). Thus the observed mean refractive index of the assemblage requires that there be no great amount of material present in the etched phase with density and refractive index even as great as those of quartz and crystalline feldspar. Thus it is likely that the etched phase is largely amorphous. This hypothesis is further supported by the observation that the material is etched by HF about as deeply as the surrounding maskelynite.

At present, there are few data from laboratory shock experiments that might permit an estimate of peak shock pressures required to form jadeite from sodic feldspar. Bytownite shocked to between 250 and 300 kb is converted to maskelynite (10); release adiabat data on oligoclase suggest complete conversion to maskelynite at peak shock pressures above about 250 kb (11); and a peak shock pressure of about 300 kb is required to form the amorphous silica glass from quartz (12). These data would suggest 250 to 300 kb as a rough estimate of the minimum shock pressures required to form

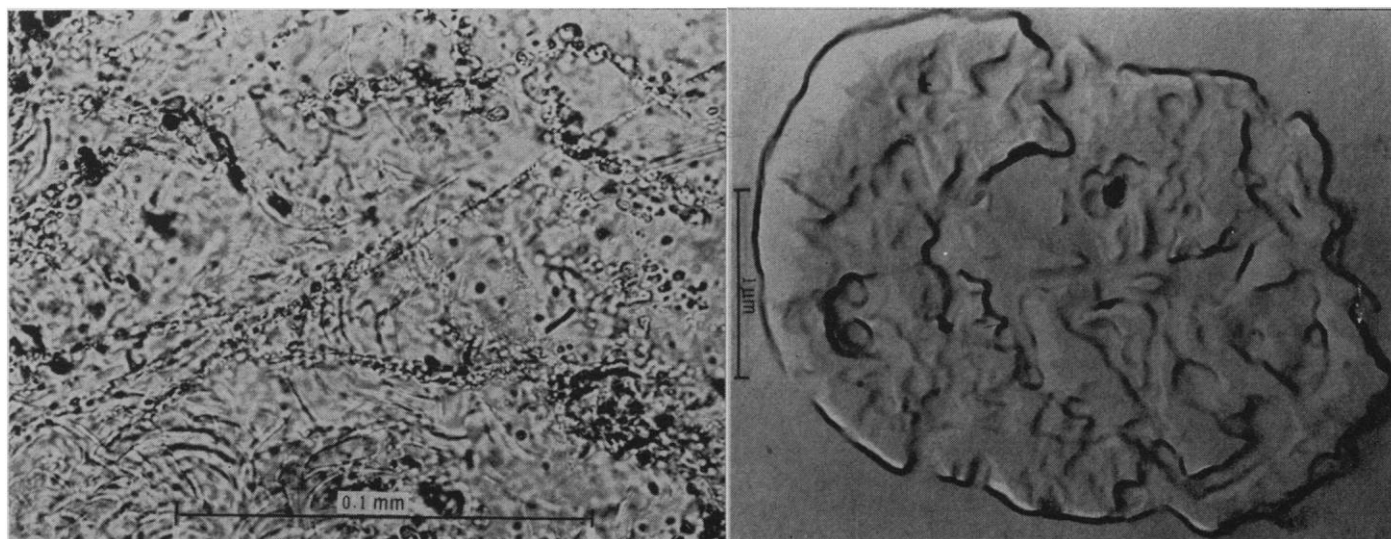


Fig. 1 (left). Irregular stringers of jadeite-bearing particles (top right and center) in maskelynite. The maskelynite also contains patches of montmorillonite and arcuate fractures that form networks at the centers of grains or patches of concentric nested arcs at grain margins (bottom left). Fig. 2 (right). Electron micrograph of jadeite-bearing particle in maskelynite. Because the shadowed replica was a negative replica, shadows are on the unetched jadeite. The etched phase forms patches and stringers within the jadeite.

jadeite. Of course, there may also be a maximum shock pressure associated with the formation of jadeite from sodic feldspar, above which other high-pressure phases are produced (13). Jadeite has not been observed as a shock product in laboratory experiments, however, and there are great uncertainties involved in extending the results of these experiments to naturally shocked rocks. In natural impact the duration of the pressure pulse may be much greater than in laboratory dynamic experiments; since the formation of jadeite is a chemical breakdown apparently requiring diffusion over distances on the order of 0.1 to 0.5  $\mu\text{m}$  (Fig. 2), the duration of the peak pressure should be an important factor in determining whether the reaction will occur and what pressure is required.

ODETTE B. JAMES

U.S. Geological Survey,  
Washington, D.C. 20242

#### References and Notes

1. The term thetomorphic was introduced by E. C. T. Chao [*Res. Geochem.* 2, 212 (1967)] to describe glasses produced from minerals by shock transformation in the solid state.
2. Origin of the Ries Crater by meteor impact has been established by the occurrence of the high-pressure polymorphs of quartz—coesite and stishovite [E. M. Shoemaker and E. C. T. Chao, *J. Geophys. Res.* 66, 3371 (1961); E. C. T. Chao and J. Littler, *Geol. Soc. Amer. Abstr.* 1962, 127 (1963)].
3. Refractive indices were determined by E. C. T. Chao and Miss J. Boreman with an interference microscope.
4. Extrapolation of the results of static high-pressure laboratory experiments indicates that jadeite can coexist with free silica at room temperatures only at pressures above 6 kb [F. Birch and P. LeCompte, *Amer. J. Sci.* 258, 209 (1960)].
5. The most common lines attributed tentatively to unidentified alteration products have  $d$ -spacings of 2.71, 2.16, 2.02, 4.00, 2.54, and 2.34 Å. Line intensities are strongest in grains that contain abundant calcite and montmorillonite and little or no jadeite.
6. H. S. Yoder, *Amer. J. Sci.* 248, 225 (1960).
7. Cell parameters were calculated and refined by computer by use of the least-squares method [D. E. Appleman and H. T. Evans,

*Jr., Geol. Soc. Amer. Spec. Pap.* 115, 8 (1968)].

8. I calculated the mean refractive index of the assemblage by assuming the following values for density (in grams per cubic centimeter) and refractive index:

Component	$\rho$	R.I.
Anorthite	2.76	1.583
Albite	2.62	1.532
Orthoclase	2.56	1.522
Quartz	2.65	1.548
Silica glass	2.20	1.460
Jadeite (pure)	3.30	1.660
Jadeite (with Ca-Al substitution for Na-Si)	3.33	1.670

In estimating refractive indices of assemblages containing impure jadeite, it is assumed that only 75 percent of the original oligoclase breaks down to jadeite +  $\text{SiO}_2$  (necessitated by the observation that jadeite forms only about half the volume of the particles). Volume relations for the four assemblages are:

Component	1	2	3	4
Jadeite	0.50	0.48	0.49	0.47
Anorthite	.25	.24	.06	.06
Albite			.20	.19
Orthoclase	.07	.07	.07	.07
Quartz	.18		.18	
Silica glass		.21		.21

9. The thetomorphic oligoclase glass in this sample has a refractive index about 0.007 higher than that of "normal" glass, but this difference is, in part, due to the presence of water (P. M. Bell and E. C. T. Chao, *Carnegie Inst. Wash. Annu. Rep.* 1969, in press).
10. D. J. Milton and P. S. De Carli, *Science* 140, 670 (1963).
11. T. J. Ahrens, C. F. Petersen, J. T. Rosenberg, *J. Geophys. Res.* 74, 2727 (1969).
12. F. Hörz, in *Shock Metamorphism of Natural Materials*, B. M. French and N. M. Short, Eds. (Mono, Baltimore, 1968), p. 243.
13. Among the possibilities are: (i) breakdown into corundum plus amorphous or crystalline silica and sodium compounds [D. H. Lindsley, *Carnegie Inst. Wash. Annu. Rep.* 65, 204 (1967)]; or (ii) transition to a dense polymorph of feldspar in which Si and Al are in octahedral coordination [A. E. Ringwood, A. F. Reid, A. D. Wadsley, *Earth Planet. Sci. Lett.* 3, 38 (1967)].
14. I am grateful to E. C. T. Chao and Miss J. Boreman of the U.S. Geological Survey for the determinations of refractive indices, to J. A. Minkin of the Geological Survey and A. J. Tousimis of Biodynamics, Inc., for the electron micrographs, and to C. Hadidioccos and P. M. Bell of the Carnegie Institution of Washington for the microprobe analysis of the maskelynite and the sample of synthetic jadeite. Research done on behalf of NASA by the U.S. Geological Survey. Publication authorized by the director, U.S. Geological Survey.

23 July 1969

are best known from Hamelin Pool, a hypersaline barred embayment forming part of Shark Bay in Western Australia (2). Ancient stromatolites are regarded by most authorities as close analogs of these modern forms. However, there has been some debate over the validity of this analogy, especially as to whether most ancient stromatolites formed within or below the tidal range, whether biological or environmental factors were dominant in determining their shapes, and whether binding and trapping of sediment by algae were exclusively responsible for their growth (3).

We now report the discovery of a diverse assemblage of algal stromatolites that grew to depths of at least 45 m below sea level on fore-reef slopes of Devonian reef complexes in Western Australia. They are believed to be products of deepwater nonskeletal algae (possibly red-pigmented cyanophytes) which trapped and bound sedimentary particles and also precipitated calcium carbonate. This discovery is of considerable significance in the environmental interpretation of ancient algal stromatolites, as it shows that they were not confined to supratidal, intertidal, and very shallow subtidal environments as has generally been supposed.

Middle and Upper Devonian reef complexes are excellently exposed along the northern margin of the Canning Basin in Western Australia (4). Reef, back-reef, fore-reef, and inter-reef facies are recognized (Fig. 1). Calcareous algae and stromatoporoids are the main reef frame-builders, and these groups are also important constituents of the back-reef facies. The algal flora is among the most diverse and abundant known from the Devonian (5). The reefs grew up to 100 m or more above the sea floor of the surrounding inter-reef basins.

Algal stromatolites occur in the reef, back-reef, and fore-reef facies (Fig. 1) but are most abundant and diverse in the fore-reef, especially in the Frasnian to Famennian Virgin Hills Formation of the Bugle Gap area. The fore-reef stromatolites grew on depositional slopes that were usually inclined at from 10° to 35°, but were occasionally as high as 55°. Stromatolitic algae played an important part in binding the fore-reef deposits, and they were responsible for maintaining the abnormally high depositional dips present in some areas. The amount of depositional dip can be determined by using

## Algal Stromatolites: Deepwater Forms in the Devonian of Western Australia

**Abstract.** *A diverse assemblage of algal stromatolites occurs in Devonian reef complexes of the Canning Basin, Western Australia. Some forms grew on fore-reef depositional slopes down to at least 45 meters below sea level and are believed to be products of deepwater nonskeletal algae. It is concluded that algal stromatolites in the stratigraphic record are not to be regarded as diagnostic evidence for deposition in very shallow water.*

Algal stromatolites have been studied in considerable detail by sedimentologists in recent years. Modern marine forms are known mainly from supratidal and intertidal environments, al-

though a few shallow subtidal occurrences have been recorded (1). They have formed through the trapping and binding of calcareous sedimentary particles by algal mats, and